Controlling Al–M Interactions in Group 1 Metal Aluminyls (M = Li, Na and K). Facile Conversion of Dimers to Monomeric and Separated Ion Pairs

Matthew J. Evans,[a] Mathew D. Anker,[a,] Michael G. Gardiner,[b] Claire L. M[c]Mullin,[c] and Martyn P. Coles[a,]**

a School of Chemical and Physical Sciences, Victoria University of Wellington, P.O. Box 600, Kelburn, Wellington, New Zealand

b Research School of Chemistry, The Australian National University, Canberra, ACT 2601, Australia

c Department of Chemistry, University of Bath, Bath, BA2 7AY, UK.

ABSTRACT

The aluminyl compounds [**M**{Al(NON^{Dipp})}]$_2$ (NON^{Dipp} = [O(SiMe$_2$NDipp)$_2$]$^{2-}$, Dipp = 2,6-*i*Pr$_2$C$_6$H$_3$), which exist as contacted dimeric pairs in both the solution- and solid-states, have been converted to monomeric ion pairs and separated ion pairs for each of the group 1 metals, **M** = Li, Na, K. The monomeric ion pairs contain discrete, highly polarized Al–**M** bonds between the aluminum and the group 1 metal, and have been isolated with monodentate (THF, **M** = Li, Na) or bidentate (TMEDA, **M** = Li, Na, K) ligands at **M**. The separated ion pairs comprise group 1 cations

that are encapsulated by polydentate ligands, rendering the aluminyl anion, $[Al(NON^{Dipp})]^-$ 'naked'. For **M** = Li, this was isolated as the $[Li(TMEDA)_2]^+$ salt directly from a solution of the corresponding contacted dimeric pair in neat TMEDA, while the polydentate [2.2.2]cryptand ligand was used to generate the separated ion pairs for the heavier group 1 metals, **M** = Na and K. This work shows that, starting from the corresponding contacted dimeric pairs, the extent of the Al–**M** interaction in these aluminyl systems can be readily controlled with appropriate chelating reagents to give monomeric ion pairs and separated ion pairs.

KEYWORDS: Contacted dimeric pair (CDP), monomeric ionic pair (MIP), separated ion pair (SIP), lithium aluminyl, sodium aluminyl, potassium aluminyl.

INTRODUCTION

Small molecule activation facilitated by main group complexes is now well established, and continues to be an active area of research.[1-6] While small molecule activation by redox inactive complexes are known,[7-8] low valent *p*-block systems are particularly effective due to their inherent ability to engage in a wide-range of oxidation and coordination reactions.[9-15] The success of these low valent main group systems to activate 'inert' substrates such as dihydrogen[16] and more recently dinitrogen,[17-18] are testament to their unusual structures and high reactivities. For aluminum-based complexes, early studies were largely restricted to neutral low valent systems (*i.e.* $(BDI^{Dipp})Al$, Cp*Al; BDI^{Dipp} = $[HC(CMeNDipp)_2]^-$).[19-23] More recently this area has been complemented by studies involving a new class of anionic aluminum compounds, aluminyl anions.[24]

Aluminyl anions are aluminum(I) complexes in which the metal center is supported by a dianionic ligand, with a group 1 metal cation present to balance the charge. To date, only six examples of aluminyl anions are known, supported by either tridentate ($[\mathbf{I}]^-$) or bidentate ($[\mathbf{II}]^-$ – $[\mathbf{VI}]^-$) ligand systems (Figure 1~~Figure 1~~).[25-30] Three distinct structural classes exist within the aluminyl family that can be defined by the degree of interaction with the group 1 metal cation. Contacted dimeric pairs (CDPs) are non-solvated dimers that can be either slipped (**M** = Li, Na) containing one strong and one weak Al–**M** bond, or symmetrical (**M** = K) with two relatively weak Al–**M** bonds. Both types are further stabilized by additional **M**···π(arene) interactions to flanking aromatic substituents of the supporting ligands. Monomeric ion pairs (MIPs) are structures in which the group 1 metal is involved in a discrete (unsupported) Al–**M** bond, with additional solvation completing the coordination sphere at **M**. Finally, separated ion pairs (SIPs) are ionic compounds in which the group 1 metal cation is fully sequestered giving a 'naked' aluminyl anion (Figure 1~~Figure 1~~).

Formatte

Formatte

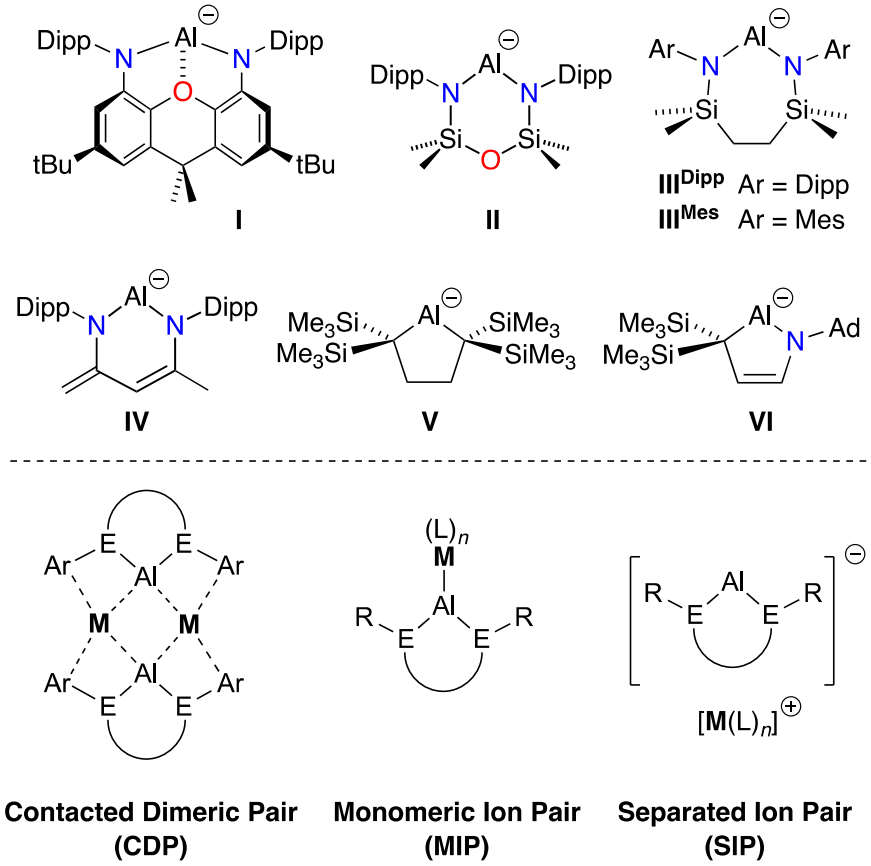

Figure 1. Top: Current family of aluminyls. Bottom: Three main structural motifs encountered in aluminyl chemistry.

The CDP structural motif is currently exclusive to the *N*-heterocyclic aluminyl anions that contain aryl substituents on the nitrogen atoms and is observed in the potassium aluminyls [**I**-K]$_2$,[25] [**II**-K]$_2$,[26] [**III**$^{\mathbf{Dipp}}$-K]$_2$,[27] [**III**$^{\mathbf{Mes}}$-K]$_2$,[31] and [**IV**-K]$_2$.[28] In contrast, the dialkyl aluminyl **V**-K(toluene)$_2$[29] was isolated as the MIP, containing a highly polarized Al–K bond and K$\cdots\pi$(arene) interactions supplied by two molecules of toluene. The cyclic alkyl amino aluminyl [**VI**][K(12-crown-4)$_2$][30] has only been reported as the SIP, with two molecules of 12-crown-4 encapsulating the potassium cation.

The CDPs provide a convenient source of the aluminyl anions from which to access the corresponding MIPs and SIPs, provided that the donor ligands that are introduced support interactions that are sufficient to overcome the K···π(arene) contacts. This has been demonstrated by the isolation of the MIP **III**$^{\mathbf{Dipp}}$-K(18-crown-6),[31] and the SIPs [**I**][K(2.2.2-crypt)],[32] [**III**$^{\mathbf{Dipp}}$][K(2.2.2-crypt)] and [**III**$^{\mathbf{Dipp}}$][K(18-crown-6)$_{1.5}$].[31] The motivation for accessing these different structural classes is more than just a curiosity, with the 'naked' aluminyl anion component of the SIPs showing increased and in some cases divergent reactivity from the corresponding CDPs. A prime example of this is observed in the cleavage of the C–H or C–C bond of benzene by CDP [**I**-K]$_2$[25] and SIP [**I**][K(2.2.2-crypt)],[32] respectively, demonstrating the significance of the group 1 metal cation in mediating the reactivity of aluminyl anion [**II**]$^-$. These 'alkali metal mediated' effects may change across the series of group 1 cations, a phenomenon that has been observed by other main group metal / group 1 metal systems.[33]

The early aluminyl systems were exclusively isolated with potassium as the counter cation. We have recently expanded this field with our report of the first lithium ([**II**-Li]$_2$) and sodium ([**II**-Na]$_2$) aluminyls, synthesized from the reduction of the aluminum(III) iodide precursor Al(NON^{Dipp})I (**II**-I) with lithium or sodium metal, respectively.[34] Both [**II**-Li]$_2$ and [**II**-Na]$_2$ were isolated as slipped CDPs with differing degrees of Al–**M** bonding between the aluminum and the two cations in the dimer (*e.g.* Al–**M** Wiberg bond indices (WBIs): [**II**-Li]$_2$ = 0.268 / 0.095; [**II**-Na]$_2$ = 0.171 / 0.093). This is in contrast to the previously reported potassium CDP [**II**-K]$_2$, for which a symmetrical CDP with equivalent Al–K interactions are observed (WBIs [**II**-K]$_2$ = 0.130 / 0.130).[26] A subsequent article reported that the attempted reduction of the aluminum iodide **I**-I with either lithium or sodium metal failed to access the aluminyls '**I**-Li' and '**I**-Na',[35] highlighting the importance of the supporting ligand framework in this area of chemistry. Furthermore, we

determined that [**II**-Li]$_2$ and [**II**-Na]$_2$ provide a facile route to the MIPs **II**-Li(Et_2O)$_2$ and **II**-Na(Et_2O)$_2$, which can be accessed by simply dissolving the CDPs in diethyl ether solvent.[34] Cleaving these dimers was shown to be reversible and equilibria consisting of the MIP and the corresponding CDP/Et_2O were observed in solution. In an alternative approach, the corresponding MIP system **I**-Li(Et_2O)$_2$ was isolated in low yield by cation exchange from [**I**-K]$_2$ using lithium iodide and diethyl ether.[35]

In this contribution, we report the synthesis and structure of the full series of monomeric ion pairs and separated ion pairs for the aluminyl anion [Al(NON^{Dipp})]$^-$ with the group 1 metals lithium, sodium and potassium. The results demonstrate our ability to mediate the position of the group 1 cation and provides a platform for studying the role that the group 1 metals contribute to the reactivity with this system.

RESULTS AND DISCUSSION

Preparation and Structure of Monomeric Ion Pairs (MIPs). Density functional theory (DFT) studies on the aluminyl systems [**II**-**M**]$_2$ (**M** = Li, Na, K) have previously shown that disruption of the CDP and formation of the bis(diethyl ether) solvated MIPs (NON^{Dipp})Al–**M**(Et$_2$O)$_2$ becomes energetically less favorable with the heavier group 1 metals, according to the order Li > Na > K. This was demonstrated by the formation of the MIPs for Li and Na, but failure to isolate the corresponding (NON^{Dipp})Al–K(Et$_2$O)$_2$ complex when [**II**-K]$_2$ was dissolved in diethyl ether.[34] Further evidence for the fine balance between the CDPs and MIPs structures was observed in the solution-state equilibria for **II**-Li(Et$_2$O)$_2$ and **II**-Na(Et$_2$O)$_2$, which were shown to co-exist with the corresponding CDPs and free diethyl ether when dissolved. To further examine the relationship between the CDP and MIP structures in the presence of different donor solvents, the aluminyl salts [**II**-**M**]$_2$ (**M** = Li, Na, K) were dissolved in THF to access the corresponding THF adducts **1**-**M** (Scheme 1).

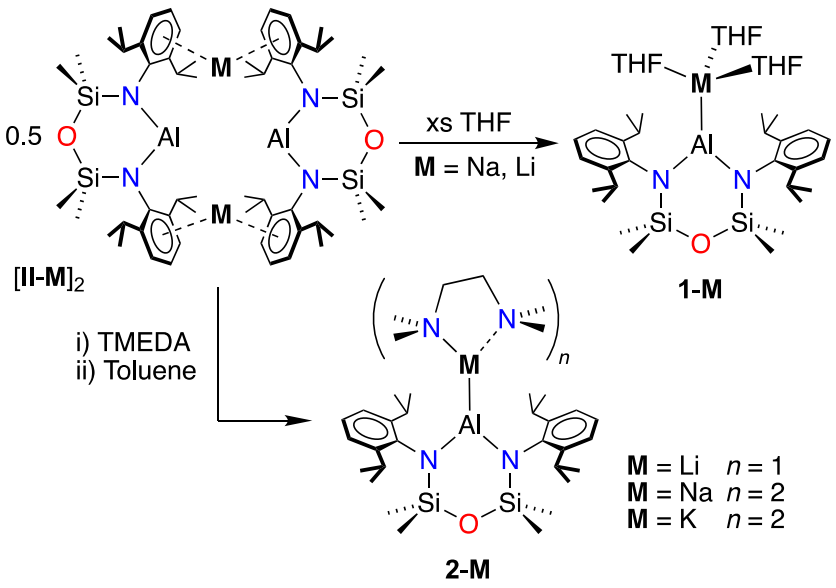

Scheme 1. Synthesis of MIPs **1**-**M** and **2**-**M** from the corresponding CDPs **II**-**M** with THF (**1**) and TMEDA (**2**). Note: [**II**-Li]$_2$ and [**II**-Na]$_2$ shown as the non-slipped CDPs.

Samples of [**II**-**M**]$_2$ (**M** = Li, Na) were dissolved in THF and the products of the reactions were crystallized from hexane (**M** = Li) or toluene (**M** = Na) at –30 °C, affording large single crystals of (NON^{Dipp})Al–Li(THF)$_3$ (**1**-Li) and (NON^{Dipp})Al–Na(THF)$_3$ (**1**-Na). The ^{1}H NMR spectra revealed a pattern for the NON^{Dipp}-substituents typical of an averaged C_{2h}-symmetry at aluminum, most evident from a singlet at δ_H 0.52 (**1**-Li) and 0.42 (**1**-Na) for the Si*Me*$_2$ groups. Multiplets were observed at δ_H 3.37 and δ_H 1.29 (**1**-Li) and δ_H 3.41 and δ_H 1.37 (**1**-Na) integrating to three equivalents of THF. These are shifted from the values for free THF in C_6D_6 (δ_H 3.57 and δ_H 1.40),[36] indicating coordination to **M** is retained in solution.

In contrast to the diethyl ether adducts **II**-Li(Et$_2$O)$_2$ and **II**-Na(Et$_2$O)$_2$, the addition of aliphatic (hexane, cyclohexane) or aromatic (benzene, toluene) solvents to **1**-Li and **1**-Na did not establish an equilibrium with the corresponding CDPs,[34] reflecting the stronger σ-donation of the THF. The increased stability of MIP **1**-Li is also evident from the ^{7}Li NMR spectrum, which shows a single resonance at δ_{Li} 3.25 (294 K, C_6D_6). This contrasts with ^{7}Li NMR data collected on a sample of isolated **II**-Li(Et$_2$O)$_2$ (294 K, C_7D_8), where two peaks are observed at δ_{Li} –2.92 and 2.68 indicating both species of the CDP : MIP equilibrium are present in solution.

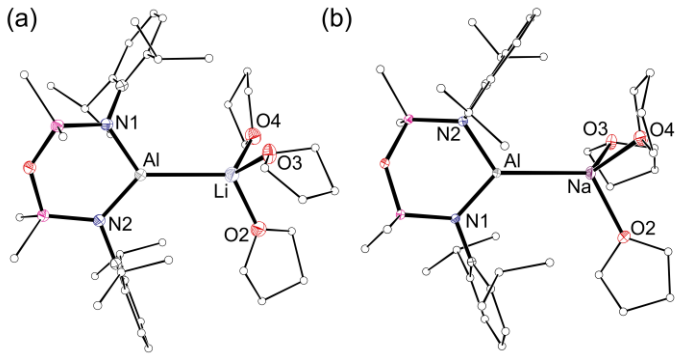

Figure 2. Displacement ellipsoid plot (30 % probability, C-atoms represented as spheres, H-atoms and disordered atoms omitted) of (a) **1**-Li and (b) **1**-Na. Selected bond length (Å) and angles (°). **1**-Li: Al–Li 2.839(5), Al–N1 1.890(2), Al–N2 1.898(2), Li–O2 1.944(5), Li–O3 2.010(5), Li–O4 1.970(5), N1–Al–N2 103.45(9). **1**-Na: Al–Na 2.9889(7), Al–N1 1.8883(13), Al–N2 1.8892(13), Na–O2 2.2723(14), Na–O3 2.3299(14), Na–O4 2.2942(14), N1–Al–N2 103.52(5).

Single crystal X-ray diffraction data confirm that **1**-Li and **1**-Na are the MIPs (NON^{Dipp})Al–**M**$(THF)_3$, containing rare examples of discrete Al–**M** bonds (Figure 2). The compounds are isostructural but not isomorphous, with three molecules of THF supporting the group 1 metal cation. In both structures, the aluminum is distorted trigonal planar (Σ_{angles} = 360°). The Al–**M** bond lengths (**1**-Li, 2.839(5) Å; **1**-Na, 2.9889(7) Å) are longer than in the previously reported lithium **II**-Li$(Et_2O)_2$ (2.767(2) Å),[34] **I**-Li$(Et_2O)_2$ (2.750(4) Å)[35] and sodium **II**-Na$(Et_2O)_2$ (3.0137(8) Å)[34] etherates, reflecting the increased coordination number at **M**, and are slightly longer than the sum of the covalent radii ($\Sigma_{Al–Li}$ = 2.49 Å; $\Sigma_{Al–Na}$ = 2.87 Å).[37]

Prior to the reports of **II**-Li$(Et_2O)_2$[34] and **I**-Li$(Et_2O)_2$,[35] a search of the 'Al–Li' fragment in the Cambridge Structural Database (CSD)[38] returned four results.[39-42] However, in all of these

examples the Al–Li 'bond' is supplemented by either bridging ligands or π-interactions. Similarly, a CSD search of the 'Al–Na' fragment returned five results (other than **II**-Na(Et_2O)$_2$) with Al–Na 'bonds'.[43-44] Therefore **1**-Li and **1**-Na join the small but growing number of compounds that have discrete (unsupported) Al–Li and Al–Na bonds.

When [K{Al(NON^{Dipp})}]$_2$ was dissolved in THF, there was no evidence for the formation of the corresponding THF adduct and we were unable to isolate a MIP from this reaction. This inspired us to test whether the bidentate donor tetramethylethylenediamine (TMEDA) would be capable of converting the CDPs to the corresponding MIPs for all three metals **M** = Li, Na, K. Dissolving samples of [**II**-**M**]$_2$ (**M** = Li, Na, K) in TMEDA afforded the corresponding adducts (NON^{Dipp})Al–Li(TMEDA) (**2**-Li) and (NON^{Dipp})Al–**M**(TMEDA)$_2$ (**2**-Na and **2**-K) on work-up (Scheme 1). For **M** = Li and K, the excess TMEDA was removed *in vacuo* and the residue dissolved in a minimum amount of toluene to form crystals of **2**-**M** at –30 °C. In the case of **M** = Na, slow evaporation of TMEDA from the solution at room temperature yielded single crystals of **2**-Na.

The ^{1}H NMR spectrum for each product revealed a singlet at δ_H 0.34 (**2**-Li), 0.54 (**2**-Na), and 0.37 (**2**-K) for the Si*Me$_2$* groups, consistent with an averaged C_{2h}-symmetry. The ^{7}Li NMR spectrum of **2**-Li shows a singlet at δ_{Li} 3.66 (C_7D_8) in a region comparable with that for the other Li MIPs (*vide supra*). However, the ^{1}H NMR resonances for the TMEDA ligand are broad at room temperature and obscured by overlap with the isopropyl methyl signals from the NON^{Dipp} ligand. Heating a sample of **2**-Li to 373 K resolves the TMEDA resonances to broad singlets at δ_H 1.50 (4H, C*H$_2$*) and δ_H 1.37 (12H, C*H$_3$*) consistent with one equivalent of TMEDA coordinated at lithium (Figure S11). The ^{1}H NMR spectra of **2**-Na and **2**-K show a single set of sharp resonances at δ_H 1.96 (8H, C*H$_2$*), δ_H 1.82 (24H, C*H$_3$*) and δ_H 2.34 (8H, C*H$_2$*), δ_H 2.11 (24H, C*H$_3$*) respectively, corresponding to two symmetrically bound TMEDA molecules.

The crystal structures of **2**-Li, **2**-Na and **2**-K confirm the formation of MIPs containing discrete Al–**M** interactions, supported by either one (**M** = Li) or two (**M** = Na, K) molecules of TMEDA (Figure 3). In each compound **2**-**M**, the aluminum is three-coordinate and occupies a distorted trigonal planar geometry defined by the NON^{Dipp}-ligand and the Al–**M** bond. Compound **2**-Li contains one TMEDA molecule bound to the lithium, whereas two are equivalents present for **2**-Na and **2**-K. The increase in ionic radii as the group descends, where Li (0.98 Å) < Na (1.33 Å) < K (1.75 Å)[45] results in a different coordination environment at the group 1 metal, with coordination numbers increasing from three (**M** = Li) to four (**M** = Na) to five (**M** = K) in the solid state.

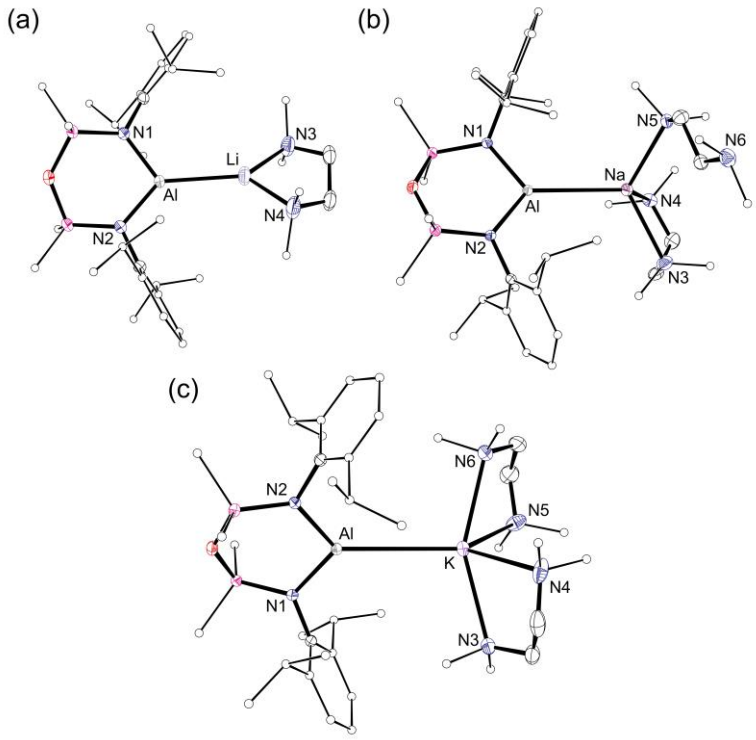

Figure 3. Displacement ellipsoid plot (30 % probability, C-atoms represented as spheres, H-atoms and disordered atoms omitted) of (a) **2**-Li, (b) **2**-Na and (c) **2**-K. Selected bond length (Å)

and angles (°). **2**-Li: Al–Li 2.669(5), Al–N1 1.874(2), Al–N2 1.877(2), Li–N3 2.044(7), Li–N4 2.036(7), N1–Al–N2 102.54(10). **2**-Na: Al–Na 3.1397(6), Al–N1 1.8951(10), Al–N2 1.9003(10), Na–N3 1.5206(13), Na–N4 2.629(8), Na–N5 2.5101(12), Na···N6 4.9413(14), N1–Al–N2 101.49(4). **2**-K: Al–K 3.6374(7), Al–N1 1.9022(17), Al–N2 1.9133(17), K–N3 2.856(2), K–N4 2.913(2), K–N5 2.979(2), K–N6 2.819(2), N1–Al–N2 101.03(7).

In compound **2**-Li, the chelation of TMEDA defines a bite angle of 89.6(3)° at the three coordinate lithium, which is considerably less than the O–Li–O angle in **II**-Li(Et_2O)$_2$ (111.91(11)°). This enables the cationic component to approach closer to the aluminyl anion, resulting in a shorter Al–Li bond length of 2.669(5) Å, equivalent to a shortening of 3.5 % and 6.0 % compared with the Al–Li bond length in **II**-Li(Et_2O)$_2$[34] and **1**-THF, respectively. The larger size of the sodium cation allows two molecules of TMEDA to be incorporated in the structure of **2**-Na. In contrast to the symmetrical binding observed in solution by NMR spectroscopy, only one molecule is bidentate with the other molecule coordinating through a single nitrogen atom (*i.e.* 'dangling'), generating what may be considered a 'Na(TMEDA)$_{1.5}$' unit. Although an η^1-coordination of TMEDA has been previously observed at lithium[46-49] and potassium,[50] the bonding of a single nitrogen donor group of TMEDA at sodium has only been structurally characterized within a bridging TMEDA ligands.[51-52] The resulting Al–Na bond in **2**-Na (3.1397(6) Å) is 4.2 % longer than in **I**-Na(Et_2O)$_2$[34] and 5.0 % longer than in **1**-Na, reflecting the more sterically encumbered environment at sodium. Compound **2**-K contains two molecules of TMEDA that are both bidentate at potassium. The Al–K bond length is intermediate between the other structurally characterized examples of discrete Al–K bonds, **III**$^{\mathbf{Dipp}}$-K(18-crown-6) (3.9133(6) Å),[31] and **V**-K(toluene)$_2$ (3.4549(5) Å).[29]

The syntheses of the THF (**1**-**M**) and TMEDA (**2**-**M**) adducts described herein demonstrate the facile access to MIPs containing discrete Al–**M** bonds that were until recently unknown. The TMEDA adducts **2**-**M** represent the first contiguous series of aluminyl MIPs involving the lighter group 1 metals Li, Na and K.

Preparation and Structure of Separated Ion Pairs (SIPs). A sample of [**II**-Li]$_2$ crystallized directly from TMEDA afforded yellow crystals, **3**. In contrast to the ^{1}H NMR spectrum of **2**-Li, the spectrum of **3** showed broad resonances at δ_H 1.87 (8H, C*H*$_2$) and δ_H 1.77 (24H, C*H*$_3$), with integration consistent with two equivalents of TMEDA. With reference to the series of compounds (NON^{Dipp})Al–**M**(TMEDA)$_n$ (**M** = Li, n = 1; **M** = Na, n = 1.5; **M** = K, n = 2) in which only one equivalent of TMEDA coordinated to Li when an Al–Li bond is present, and taking the size of the lithium cation into account, we initially interpreted these data as equivalent to the separated ion pair, [Li(TMEDA)$_2$][Al(NON^{Dipp})]. The ^{7}Li NMR spectrum of **3** in C_6D_6 however shows a singlet at δ_{Li} 3.50, close to the values observed for the MIPs **II**-Li(Et$_2$O)$_2$ and **2**-Li. This is shifted to higher frequency than has been previously observed for the [Li(TMEDA)$_2$]$^+$ cation in C_6D_6 (δ_{Li} 0.13 – 2.0),[53-55] although deviation from regular coordination geometries at lithium has been linked to unexpected chemical shifts.[56] Furthermore, evidence for the facile loss of one equivalent of TMEDA from **3** was forthcoming when a sample was crystallized from toluene, affording crystals of the MIP **2**-Li.

We therefore considered a possible solution-state equilibrium between the separated ion pair **3** and the monomeric ion pairs **3'** (with an intermediate 'Li(TMEDA)$_{1.5}$' group, equivalent to the sodium environment observed in the solid-state for **2**-Na) and **2**-Li in solution, which contribute to the broad TMEDA resonances in the ^{1}H NMR spectrum and the low-field resonance in the ^{7}Li

NMR spectrum (Scheme 2). The addition of excess (5 equivalents) of TMEDA did not cause significant changes ^{7}Li NMR spectrum (δ_{Li} 3.41), although broad resonances at δ_{H} 2.11 and 1.94 in the ^{1}H NMR spectrum are suggestive of exchange (Figure S38). Unfortunately, attempts to observe the proposed species in solution state using variable temperature ^{1}H NMR spectroscopy failed to clearly resolve the peaks for the separate species across the temperature range 193 K – 363 K (Figure S19). The ^{7}Li NMR spectra over the same temperature range indicated the presence of multiple lithium environments (Figure S20), but no firm conclusions as to the exact nature of these species can be reached from these data.

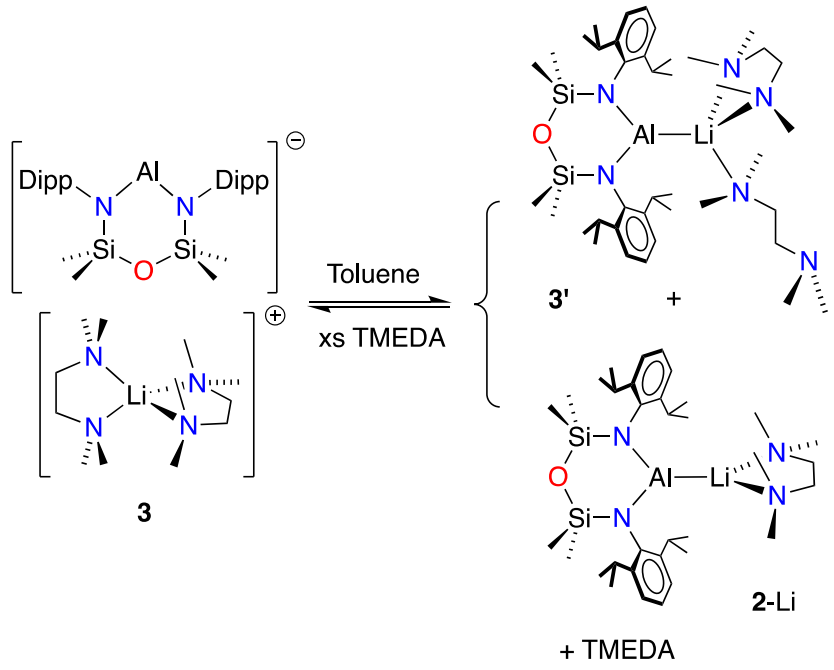

Scheme 2. Proposed solution-state equilibrium between SIP **3** and MIPs **3'** and **2**-Li.

The solid-state structure of **3** was confirmed as [Li(TMEDA)$_2$][Al(NON^{Dipp})] by an X-ray crystallographic study, representing the first example of an SIP involving a lithium aluminyl

(Figure 4). The structure contains two crystallographically inequivalent cation / anion pairs, one of which lies on a mirror plane and is disordered about this symmetry element. There are no contacts between the cationic and anionic components in each case, indicated by the aluminum to lithium distances of 5.309(5) Å and 5.553(6) Å, confirming a strictly two coordinate aluminum center in the anion $[Al(NON^{Dipp})]^-$.

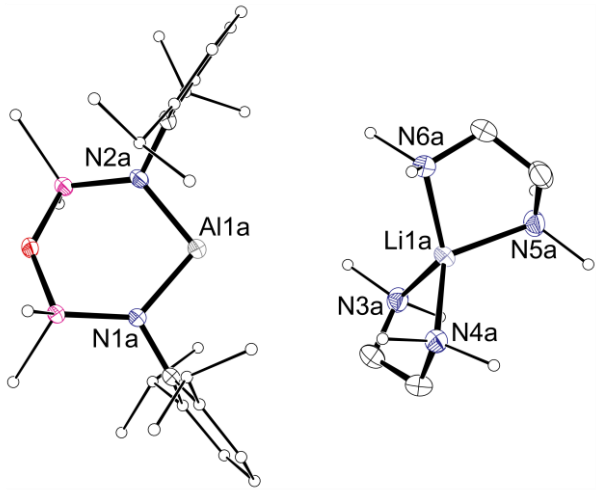

Figure 4. Displacement ellipsoid plot (30 %, C-atoms reduced for clarity, H-atoms and disordered atoms omitted) of one of the independent molecules of **3**. Selected bond lengths (Å) and angles (°) {equivalent value for second independent molecule}: Al1a···Li1a 5.309(5) {5.553(6)}, Al1a–N1a 1.933(2) {1.914(3)}, Al1a–N2a 1.923(2) {1.930(3)}, Li1a–N3a 2.120(6) {2.11(2)}, Li1a–N4a 2.107(6) {2.13(2)}, Li1a–N5a 2.118(6) {2.103(8)}, Li1a–N6a 2.131(6) {2.130(8)}, N1a–Al1a–N2a 100.24(10) {103.34(13)}.

Attempts to isolate the corresponding potassium and sodium analogues of **3** directly from TMEDA solution were not successful. We therefore adopted an established method for sequestering the heavier group 1 metals by the addition of a polydentate cryptand ligand. In the case of potassium, this has been successful in the isolation of SIPs [**I**][K(2.2.2-crypt)][32] and [**III**$^{\mathbf{Dipp}}$][K(2.2.2-crypt)].[31]

The reaction between [2.2.2]cryptand and CDPs [**II**-Na]$_2$ and [**II**-K]$_2$ in benzene initially gave immiscible liquid : liquid phase separated mixtures (clathrates) from which the corresponding SIPs [Na(2.2.2)crypt][Al(NON^{Dipp})] (**4**-Na) and [K(2.2.2)crypt][Al(NON^{Dipp})] (**4**-K) were isolated (Scheme 3). Agitation of the clathrate formed with [**II**-K]$_2$ gave bright yellow crystals of **4**-K in high yields. In contrast, crystallization of **4**-Na could only be achieved from THF. This procedure is problematic because both **4**-Na and **4**-K decompose slowly in THF to form a mixture of unknown products that are poorly soluble in aliphatic or aromatic solvents (Figure S25). For **4**-Na, this was reflected in the relatively low yield (32 %) obtained after crystallization. Single crystal X-ray diffraction data confirmed the formation of SIPs for **4**-K and **4**-Na (Figure 5).

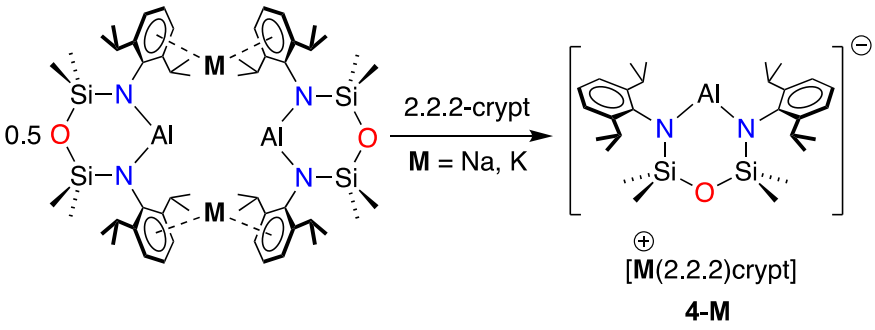

Scheme 3. Synthesis of SIPs **4**-**M** (**M** = Na, K) from the corresponding CDPs. Note: [**II**-Na]$_2$ shown as the non-slipped CDP.

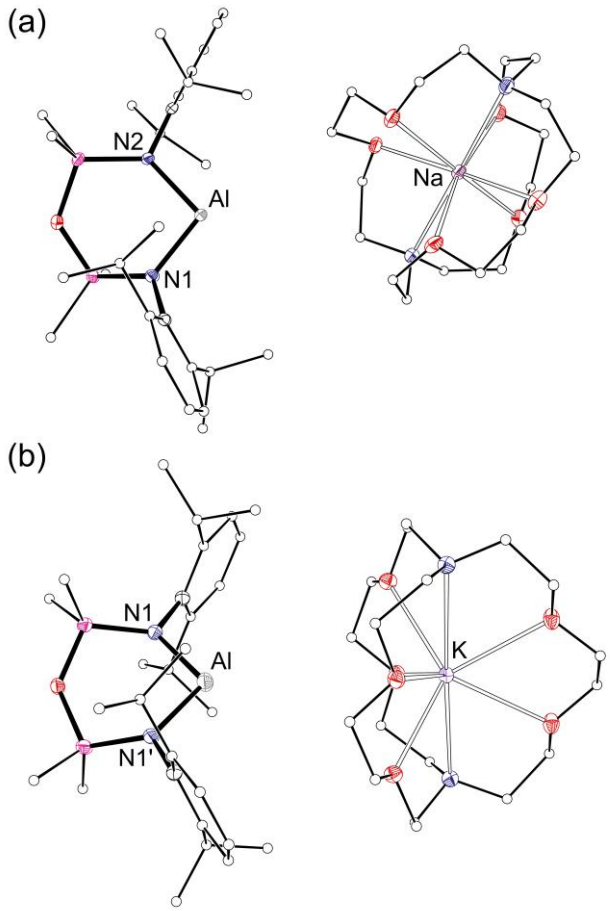

Figure 5. Displacement ellipsoid plot (30 %, C-atoms reduced for clarity, H-atoms and THF solvate (**4**-Na) omitted) of (a) **4**-Na and (b) **4**-K (' = 1-*x*, *y*, ½–*z*). Selected bond lengths (Å) and angles (°). **4**-Na: Al···Na' 6.630(6), Al–N1 1.9147(11), Al–N2 1.9391(11), N1–Al–N2 98.89(5). (°): **4**-K: Al···K 5.7066(9), Al–N1 1.9341(13), N1–Al–N1' 100.43(1).

As for the lithium SIP **3**, there are no contacts between the cationic and anionic components in **4**-Na and **4**-K, indicated by the shortest Al···Na and Al···K distances of 6.630(6) Å and 5.7066(9) Å, respectively. The Al–N bond lengths and N–Al–N angle are similar to those noted in **3** (Table 1), consistent with a similar electronic structure at aluminum for the $[Al(NON^{Dipp})]^-$ anion in the

SIPs for all group 1 metals. Compound **4**-K adds to the growing number of potassium aluminyl SIPs,[30-32] while **4**-Na represents the first example of a SIP involving the sodium cation. These systems provide a series of 'naked' aluminyl anions, where the cation has essentially no bonding interactions to the anionic moiety.

COMPUTATIONAL STUDY

A density functional theory (DFT) study comparing the natural charges at aluminum (q_{Al}) for the compounds described in this study shows that upon formation of the Al–Li bond in the MIPs, the calculated charges decrease from a value of +1.059 for the CDP [**II**-Li]$_2$ (with two Al–Li interactions) to +0.877 and +0.914 for **II**-Li(Et$_2$O)$_2$ and **1**-Li, respectively (Table 1**)**. A further reduction in the positive charge at Al is noted for the non-coordinated anion [Al(NON^{Dipp})]$^-$, with the value of +0.702 reflecting the localization of electron density at this atom. Comparing with the natural charges at the group 1 metal **M** ($q_{\mathbf{M}}$) there is a general trend for a greater difference Δq (*i.e.* a more polar bond) to exist with Al–Li systems within each class of compound.

Further analysis of NBO data shows Al–**M** covalent bonds within the slipped CDPs [**II**-Li]$_2$ and [**II**-Na]$_2$ that are predominantly derived from Al orbitals (83.30 % - 89.93 %) and composed of high s-character (77.87% - 79.10%). In contrast there is no covalent bond interaction between Al and K in the symmetrical CDP [**II**-K]$_2$, with electron density located in a lone-pair at Al with high s-character (83.13 %). Of the monomeric Al–**M**(solvent)$_n$ adducts, only **2**-Li contains a bond between Al and Li such as those observed in the [**II**-M]$_2$ dimer structures, composed of 81.91 % Al orbitals with 78.11 % s-character. This is likely related to the short Al–Li bond in **2**-Li (2.669(5) Å) when compared with the Et$_2$O (2.767(2) Å) and THF (2.839(5) Å) adducts. The Al–**M** interactions in the remaining MIPs do not contain formal covalent bonds and instead a lone pair is

observed on the aluminum center, as noted in [**II**-K]$_2$. The aluminum lone-pairs all possess high s-character (79.74 % - 82.63 %), although there are no strong correlations between the extent of this hybridization and the group 1 metal **M**. Finally, we note that the lone-pair calculated for the "naked" aluminyl anion contains a higher percentage of s-character (88.14 %), reflecting an energetically more stable s-rich hybridization.

CONCLUSIONS

In summary, we have demonstrated the facile conversion of the [**M**{Al(NON^{Dipp})}]$_2$ aluminyls into MIPs containing discrete Al–**M** interactions, and SIPs that comprise a 'naked' aluminyl anion with an encapsulated cation. The lithium (**1**-Li) and sodium (**1**-Na) MIPs can be isolated as THF adducts from the corresponding CDPs, while the use of TMEDA permitted the isolation of a full series of MIPs (**2**-**M**). Recrystallization of the lithium CDP directly from TMEDA afforded the lithium SIP (**3**), which may retain Al···Li interactions in solution. The complete encapsulation of the potassium and sodium cations with 2.2.2-crypt generated the corresponding SIPs (**4**-K and **4**-Na) in which no cation:anion interactions are present. These species were unstable in THF, indicating the important role that the Al···M interactions have in stabilizing the aluminyl anions in the CDP and SIP structures. We have therefore demonstrated a high degree of control over the extent to which the group 1 metal interacts with the aluminum anion in a series of aluminyl compounds. Considering previous examples of divergent chemistry observed for the different aluminyl structural types, these compounds will form the foundation for further studies into the reactivity of the aluminyl anion, [Al(NON^{Dipp})]$^-$.

Table 1 Selected natural charges and bond / lone pair occupancy for the $[Al(NON^{Dipp})]^-$ anion associated with CDPs [**II**-**M**]$_2$ (**M** = Li, Na, K), MIPs **II**-**M**$(Et_2O)_2$ (**M** = Li, Na), **1**-**M** (**M** = Li, Na) and **2**-**M** (**M** = Li, Na, K) and the SIP **3**. The values for the aluminum(III) iodide, $Al(NON^{Dipp})I$, have been included for comparison.

Compound	**Classification**	**Natural Charge at Al (q_{Al})**	**Natural Charge at M (q_M)**	**Δq ($q_{Al} - q_M$)**	**Al Bond / Lone Pair Occupancy (%)**	
					s	**p**
$Al(NON^{Dipp})I$	Al(III)	1.677	-		-	-
[**II**-Li]$_2$	CDP (slipped)	1.058 and 1.060	0.240 and 0.285	0.818 and 0.775	79.10 * (83.30%) 78.44 * (84.42%)	20.86 * 21.52 *
[**II**-Na]$_2$	CDP (slipped)	0.940 and 0.940	0.414 and 0.414	0.526	77.92 * (89.93%) 77.87 * (86.15%)	22.04 * 22.08 *
[**II**-K]$_2$	CDP	0.897 and 0.897	0.503 and 0.502	0.394	83.13 83.13	16.78 16.78
II-Li$(Et_2O)_2$	MIP/Et_2O	0.877	0.460	0.417	79.74	20.22
II-Na$(Et_2O)_2$	MIP/Et_2O	0.836	0.551	0.285	79.74	20.20
1-Li	MIP/THF	0.914	0.435	0.479	82.63	17.34
1-Na	MIP/THF	0.836	0.568	0.268	81.75	18.18
2-Li	MIP/TMEDA	0.901	0.436	0.465	78.11 * (81.91%)	21.85 *
2-Na	MIP/TMEDA	0.859	0.465	0.394	81.01	18.95
2-K	MIP/TMEDA	0.801	0.563	0.238	82.24	17.71
[**II**]$^{-a}$	SIP/TMEDA	0.702	-		88.14	11.8

a Coordinates taken from the $[Al(NON^{Dipp})]^-$ component of **3**

* These values are from a BD bond orbital not a LP bond orbital

EXPERIMENTAL

General Experimental Procedures. All manipulations were performed under dry argon using standard Schlenk-line techniques, or in a conventional nitrogen-filled glovebox. Hexane, toluene, diethyl ether (Et_2O), and tetrahydrofuran (THF) were obtained from a PureSolv MD 5 system and stored over activated 5Å molecular sieves for 24 hours prior to use. NMR spectra were recorded using a Jeol JNM-ECZ500S 500 MHz spectrometer equipped with a ROYAL digital auto tune probe S, operating at 500.1 (^{1}H), 125.8 (^{13}C) 194.4 (^{7}Li), 130.3 (^{27}Al) MHz. Spectra were recorded at 294 K (unless stated otherwise) and proton and carbon chemical shifts were referenced internally to residual solvent resonances. Coupling constants are quoted in Hz. Elemental analyses were carried out by the Elemental Analysis Service at London Metropolitan University. Despite our best attempts, we were unable to obtain results consistent with the expected formulae for the solvated compounds **1**-Li, **1**-Na, **2**-Li, **2**-Na and **2**-K (Table S4).[57] We attribute this to the sensitivity of the compounds to moisture and oxygen and potential issues caused by sample preparation for transport (flame-sealed under vacuum in glass ampoules, which likely caused (partial) loss of coordinated Et_2O or TMEDA, facilitating decomposition). [**M**{Al(NON^{Dipp})}]$_2$, ([**II**-**M**]$_2$: **M** = Li,[34] Na[34] and K[26]) were prepared according to literature procedures. TMEDA was dried over CaH_2, distilled under argon and stored over activated 5 Å molecular sieves. All other chemicals were purchased from Sigma-Aldrich and used without further purification.

Preparation of (NON^{Dipp})Al–Li(THF)$_3$ (1-Li). A sample of [Li{Al(NON^{Dipp})}]$_2$ ([**II**-Li]$_2$, 60 mg, 0.12 mmol) was dissolved in THF (~5 mL) to give a bright yellow solution. The solvent was removed *in vacuo* and the residue dissolved in hexane to give a colourless solution. Crystals were grown from a hexane (~1 mL) solution stored at -30 ℃. Yield 52 mg, 61 %. ^{1}H NMR (C_6D_6): δ

7.14 (d, *J* = 7.6, 4H, C_6H_3), 6.95 (t, *J* = 7.6, 2H, C_6H_3), 4.32 (sept, *J* = 6.8, 4H, C*H*Me$_2$), 3.37 (m, 36H, THF OCH_2CH$_2$), 1.48 (d, *J* = 6.8, 12H, CHMe_2), 1.40 (d, *J* = 6.8, 12H, CHMe_2), 1.29 (m, 36H, THF OCH$_2$CH_2), 0.52 (s, 12H, SiMe_2). $^{13}C\{^1H\}$ NMR (C_6D_6): δ 147.3, 147.1, 123.1, 121.8 (C_6H_3), 68.5 (THF O*C*H$_2$CH$_2$), 27.8 (*C*HMe$_2$), 26.5 (CHMe_2), 25.4 (THF OCH$_2$*C*H$_2$), 24.4 (CHMe_2), 3.4 (SiMe_2). ^{7}Li NMR (C_6D_6): δ 3.25 (br s).

Preparation of (NON^{Dipp})Al–Na(THF)$_3$ (1-Na). A sample of [Na{Al(NON^{Dipp})}]$_2$ ([**II**-Na]$_2$, 58 mg, 0.11 mmol) was dissolved in THF (~5 mL) to give a colorless solution. The solvent was reduced *in vacuo* and the resulting residue dissolved in toluene. Crystals were grown from a toluene solution (~1 mL) stored at –30 ℃. Yield 43 mg, 53 %. ^{1}H NMR (C_6D_6): δ 7.04 (d, *J* = 7.6, 4H, C_6H_3), 6.89 (t, *J* = 7.6, 2H, C_6H_3), 4.03 (br sept, 4H, C*H*Me$_2$), 3.41 (m, 12H, THF OCH_2CH$_2$), 1.37 (m, 12H, THF OCH$_2$CH_2), 1.33 (d, *J* = 6.8, 12H, CHMe_2), 1.22 (d, *J* = 6.8 , 12H, CHMe_2), 0.42 (s, 12H, SiMe_2). $^{13}C\{^1H\}$ NMR (C_6D_6): δ 147.8, 146.4, 123.2, 122.6 (C_6H_3), 67.8 (THF OCH$_2$CH$_2$), 27.6 (*C*HMe$_2$), 26.2 (CHMe_2), 25.7 (THF OCH$_2$*C*H$_2$), 24.4 (CHMe_2), 3.4 (SiMe_2).

Preparation of Al(NON^{Dipp})–Li(TMEDA) (2-Li). A solution of TMEDA (~5 mL, excess) was added to a crystalline sample of [Li$_2${Al(NON^{Dipp})}]$_2$ ([**II**-Li]$_2$, 80 mg, 0.15 mmol) to give a yellow solution. The solvent was reduced *in vacuo* and the resulting residue dissolved in toluene. Crystals were obtained from the storage of a toluene (~1 mL) solution at –30 ℃ for 18 hours. Yield 35 mg, 36 %. ^{1}H NMR (C_6D_6): δ 7.18 (d, *J* = 7.5, 4H, C_6H_3), 7.03 (t, *J* = 7.5, 2H, C_6H_3), 4.26 (sept, *J* = 6.7, 4H, C*H*Me$_2$), 1.47 (d, *J* = 6.7, 12H, CHMe_2), 1.50 – 1.25 (br, 16H, TMEDA CH_2 and CH_3)*, 1.39 (d, *J* = 6.7, 12H, CHMe_2), 0.54 (s, 12H, SiMe_2). * resonances overlap with CHMe_2 peaks. $^{13}C\{^1H\}$ NMR (C_6D_6): δ 147.3, 146.7, 123.1, 121.8 (C_6H_3), 56.0 (br, TMEDA *C*H$_2$), 44.5 (br,

TMEDA *C*H$_3$), 27.3 (*C*HMe$_2$), 26.5, 23.8 (CH*Me$_2$*), 3.5 (Si*Me$_2$*). ^{1}H NMR (C$_7$D$_8$, 373 K): δ 7.06 (d, *J* = 7.6, 4H, C$_6$*H$_3$*), 6.89 (t, *J* = 7.6, 2H, C$_6$*H$_3$*), 4.14 (sept, *J* = 6.8, 4H, C*H*Me$_2$), 1.50 (s, 4H, TMEDA C*H$_2$*), 1.45 (s, 12H, TMEDA C*H$_3$*), 1.36 (d, *J* = 6.8, 12H, CH*Me$_2$*), 1.31 (d, *J* = 6.8, 12H, CH*Me$_2$*), 0.34 (s, 12H, Si*Me$_2$*).^{1}H NMR (C$_7$D$_8$): δ 7.11 (d, *J* = 7.6, 4H, C$_6$*H$_3$*), 6.96 (t, *J* = 7.6, 2H, C$_6$*H$_3$*), 4.20 (sept, *J* = 6.8, 4H, C*H*Me$_2$), 1.43 (d, *J* = 6.8, 12H, CH*Me$_2$*), 1.38 – 1.28 (br, 16H, TMEDA C*H$_2$* and C*H$_3$*), 1.35 (d, *J* = 6.8, 12H, CH*Me$_2$*), 0.44 (s, 12H, Si*Me$_2$*). ^{13}C{^{1}H} NMR (C$_7$D$_8$): δ 147.2, 146.6, 123.0, 121.8 (*C$_6$*H$_3$), 55.7 (TMEDA *C*H$_2$), 44.1 (TMEDA *C*H$_3$), 27.7 (*C*HMe$_2$), 26.5, 24.4 (CH*Me$_2$*), 3.4 (Si*Me$_2$*). ^{1}H NMR (C$_7$D$_8$, 373 K): δ 7.06 (d, *J* = 7.6, 4H, C$_6$*H$_3$*), 6.89 (t, *J* = 7.6, 2H, C$_6$*H$_3$*), 4.14 (sept, *J* = 6.8, 4H, C*H*Me$_2$), 1.50 (s, 4H, TMEDA C*H$_2$*), 1.45 (s, 12H, TMEDA C*H$_3$*), 1.36 (d, *J* = 6.8, 12H, CH*Me$_2$*), 1.31 (d, *J* = 6.8, 12H, CH*Me$_2$*), 0.34 (s, 12H, Si*Me$_2$*). ^{7}Li{^{1}H} NMR (C$_7$D$_8$): δ 3.66.

Preparation of Al(NON^{Dipp})–Na(TMEDA)$_2$ (2-Na). A solution of TMEDA (~5 mL, excess) was added to a crystalline sample of [Na{Al(NON^{Dipp})}]$_2$ ([**II**-Na]$_2$, 72 mg, 0.14 mmol) to give a colourless solution. Crystals were obtained *via* slow evaporation from a TMEDA solution at room temperature. Yield 81 mg, 78 %. ^{1}H NMR (C$_6$D$_6$): δ 7.19 (d, *J* = 7.6, 4H, C$_6$*H$_3$*), 6.99 (t, *J* = 7.6, 2H, C$_6$*H$_3$*), 4.33 (sept, *J* = 6.8, 4H, C*H*Me$_2$), 1.96 (s, 8H, TMEDA C*H$_2$*), 1.82 (s, 24H, TMEDA C*H$_3$*), 1.48 (d, *J* = 6.8, 12H, CH*Me$_2$*), 1.45 (d, *J* = 6.8, 12H, CH*Me$_2$*), 0.54 (s, 12H, Si*Me$_2$*). ^{13}C{^{1}H} NMR (C$_6$D$_6$): δ 147.3, 147.2, 123.1, 121.9 (*C$_6$*H$_3$), 57.5, (TMEDA *C*H$_2$), 45.6 (TMEDA *C*H$_3$), 27.8 (*C*HMe$_2$), 26.8, 24.5 (CH*Me$_2$*), 3.6 (Si*Me$_2$*).

Preparation of Al(NON^{Dipp})–K(TMEDA)$_2$ (2-K). A solution of TMEDA (~5 mL, excess) was added to a crystalline sample of [K$_2${Al(NON^{Dipp})}]$_2$ ([**II**-K]$_2$, 90 mg, 0.16 mmol) to give an

insoluble white suspension. The suspension was dried *in vacuo* and redissolved in toluene (~2 mL) to give a yellow solution. Crystals were obtained from storage of the toluene solution at –30 ℃ for 18 hours. Yield 95 mg, 74 %. ^{1}H NMR (C_6D_6): δ 6.90 (d, J = 7.6, 4H, C_6H_3), 6.74 (t, J = 7.6, 2H, C_6H_3), 4.01 (sept, J = 7.0, 4H, C*H*Me$_2$), 2.34 (s, 8H, TMEDA CH_2), 2.11 (s, 24H, TMEDA CH_3), 1.27 (d, J = 6.8, 12H, CHMe_2), 1.10 (d, J = 6.8, 12H, CHMe_2), 0.37 (s, 12H, SiMe_2). ^{13}C{^{1}H} NMR (C_6D_6): δ 148.8, 148.6, 123.1, 122.4 (C_6H$_3$), 58.4, (TMEDA CH$_2$), 46.0 (TMEDA CH$_3$), 27.5 (CHMe$_2$), 25.6, 24.2 (CHMe_2), 3.4 (SiMe_2).

Preparation of [Li(TMEDA)$_2$][Al(NON^{Dipp})] (3). A solution of TMEDA (~3 mL, excess) was added to a crystalline sample of [Li$_2${Al(NON^{Dipp})}]$_2$ ([**II**-Li]$_2$, 120 mg, 0.23 mmol) to give a yellow solution. Storage of the TMEDA solution at –30 ℃ for 18 hours yielded orange crystals. Yield 61 mg, 35 %. Anal calc'd for $C_{40}H_{78}AlLiN_6OSi_2$ (*925.43 g mol^{-1}*): C, 64.13; H, 10.49; N, 11.22. Found: C, 64.26; H, 10.33; N, 10.32. ^{1}H NMR (500 MHz, C_6D_6) δ 7.18 (d, J = 7.6, 4H, C_6H_3), 7.03 (t, J = 7.6, 2H, C_6H_3), 4.26 (sept, J = 6.8, 4H, C*H*Me$_2$), 1.87 (s, 8H, TMEDA CH_2), 1.77 (s, 24H, TMEDA CH_3), 1.46 (d, J = 6.8, 12H, CHMe_2), 1.39 (d, J = 6.8, 12H, CHMe_2), 0.52 (s, 12H, SiMe_2). ^{13}C{^{1}H} NMR (C_6D_6): δ 147.3, 146.6, 123.1, 121.8 (C_6H$_3$), 57.2 (TMEDA CH$_2$) 45.3 (TMEDA CH$_3$), 27.8 (CHMe$_2$), 26.5, 24.5 (CHMe_2), 3.5 (SiMe_2). ^{7}Li NMR (C_6D_6): δ 3.50.

Preparation of [Na(2.2.2-crypt)][Al(NON^{Dipp})] (4-Na). A solution of [Na{Al(NON^{Dipp})}]$_2$ ([**II**-Na]$_2$, 78 mg, 0.15 mmol) was added to a solution of [2.2.2]cryptand (54 mg, 0.15 mmol) in benzene to give a yellow dispersion. The solvent was reduced *in vacuo* and the residue dissolved in THF (~3 mL). The resulting solution was left at room temperature to give pale yellow crystals *via* slow evaporation. Yield 42 mg, 32 %. Anal calc'd for $C_{46}H_{82}AlKN_4O_7Si$ (value for loss of THF solvate

from isolated crystals, *909.32 g mol*$^{-1}$): C, 60.76; H, 9.09; N, 6.16. Found: C, 60.73; H, 8.98; N, 5.62. ^{1}H NMR (500 MHz, THF-D$_8$): δ 6.84 (d, J = 7.6, 4H, C$_6$*H$_3$*), 6.67 (t, J = 7.6, 2H, C$_6$*H$_3$*), 4.19 (sept, J = 6.8, 4H, C*H*Me$_2$), 3.51 (s, 12H, crypt-C*H$_2$*), 3.49 – 3.46 (m, 12H, crypt-C*H$_2$*), 2.58 – 2.52 (m, 12H, crypt-C*H$_2$*), 1.22 (d, J = 6.8, 6H, CH*Me$_2$*), 1.20 (d, J = 6.8, 6H, CH*Me$_2$*), 1.13 (d, J = 6.8, 12H, CH*Me$_2$*), 0.02 (s, 6H, Si*Me$_2$*), –0.01 (s, 6H, Si*Me$_2$*). ^{13}C{^{1}H} NMR (THF-D$_8$): δ 148.5, 148.1, 147.8, 123.1, 123.0, 120.8 (*C$_6$*H$_3$), 69.4, 68.5, 53.8 (crypt-*C*H$_2$), 27.7 (*C*HMe$_2$), 26.4, 26.3, 25.9 (CH*Me$_2$*), 3.3, 2.9 (Si*Me$_2$*).

Preparation of [K(2.2.2-crypt)][(NON^{Dipp})Al] (4-K). A solution of [K{Al(NON^{Dipp})}]$_2$ ([**II**-K]$_2$, 103 mg, 0.19 mmol) was added to a solution of [2.2.2]cryptand (71 mg, 0.19 mmol) in benzene to give an orange-yellow clathrate. Upon standing, bright yellow crystals separate from the clathrate. Yield 173 mg, 99 %. Anal calc'd for C$_{46}$H$_{82}$AlKN$_4$O$_7$Si (*925.43 g mol*$^{-1}$): C, 59.70; H, 8.93; N, 6.05. Found: C, 60.83; H, 8.98; N, 5.82. ^{1}H NMR (THF-D$_8$): δ 6.88 (d, J = 7.6, 4H, C$_6$*H$_3$*), 6.64 (t, J = 7.6, 2H, C$_6$*H$_3$*), 4.11 (sept, J = 6.8, 4H, C*H*Me$_2$), 3.49 (s, 12H, crypt-C*H$_2$*), 3.47 – 3.44 (m, 12H, crypt-C*H$_2$*), 2.50 – 2.45 (m, 12H, crypt-C*H$_2$*), 1.24 (d, J = 6.8, 12H, CH*Me$_2$*), 1.17 (d, J = 6.8, 12H, CH*Me$_2$*), –0.03 (s, 12H, Si*Me$_2$*). ^{13}C{^{1}H} NMR (THF-D$_8$): δ 149.8, 147.6, 122.5, 120.4 (*C$_6$*H$_3$), 71.4, 68.6, 55.0 (crypt-*C*H$_2$), 28.1 (*C*HMe$_2$), 27.2, 24.6 (CH*Me$_2$*), 3.8 (Si*Me$_2$*).

ASSOCIATED CONTENT

Supporting Information. The following files are available free of charge:

NMR spectra (PDF)

X-ray crystallographic data (CIF)

AUTHOR INFORMATION

Corresponding Author

Martyn P. Coles. Email: martyn.coles@vuw.ac.nz; orcid.org/0000-0003-3558-271X

Authors

Matthew J. Evans; orcid.org/0000-0002-5383-3220

Mathew D. Anker; orcid.org/0000-0003-0414-7635

Michael G. Gardiner; orcid.org/0000-0001-6373-4253

Claire L. McMullin; orcid.org/0000-0002-4924-2890

Author Contributions

The manuscript was written through contributions of all authors. All authors have given approval to the final version of the manuscript.

Funding Sources

MPC and MJE acknowledge Government funding from the Marsden Fund Council, managed by Royal Society Te Apārangi (Grant Number: MFP-VUW2020). The authors wish to acknowledge a Victoria University of Wellington Doctoral Scholarship (MJE).

References

(1) Weetman, C.; Inoue, S. The Road Travelled: After Main-Group Elements as Transition Metals. *ChemCatChem* **2018**, *10*, 4213-4228.

(2) Yadav, S.; Saha, S.; Sen, S. S. Compounds with Low-Valent p-Block Elements for Small Molecule Activation and Catalysis. *ChemCatChem* **2016**, *8*, 486-501.

(3) Revunova, K.; Nikonov, G. I. Main Group Catalysed Reduction of Unsaturated Bonds. *Dalton Trans.* **2015**, *44*, 840-866.

(4) Mandal, S. K.; Roesky, H. W. Group 14 Hydrides with Low Valent Elements for Activation of Small Molecules. *Acc. Chem. Res.* **2012**, *45*, 298-307.

(5) Power, P. P. Interaction of Multiple Bonded and Unsaturated Heavier Main Group Compounds with Hydrogen, Ammonia, Olefins, and Related Molecules. *Acc. Chem. Res.* **2011**, *44*, 627-637.

(6) Power, P. P. Main-Group Elements as Transition Metals. *Nature* **2010**, *463*, 171-177.

(7) Hill, M. S.; Liptrot, D. J.; Weetman, C. Alkaline Earths as Main Group Reagents in Molecular Catalysis. *Chem. Soc. Rev.* **2016**, *45*, 972-988.

(8) Kobayashi, S.; Yamashita, Y. Alkaline Earth Metal Catalysts for Asymmetric Reactions. *Acc. Chem. Res.* **2011**, *44*, 58-71.

(9) Chu, T.; Nikonov, G. I. Oxidative Addition and Reductive Elimination at Main-Group Element Centers. *Chem. Rev.* **2018**, *118*, 3608-3680.

(10) Hadlington, T. J.; Driess, M.; Jones, C. Low-Valent Group 14 Element Hydride Chemistry: Towards Catalysis. *Chem. Soc. Rev.* **2018**, *47*, 4176-4197.

(11) Roesky, H. W. Chemistry of Low Valent Silicon. *J. Organomet. Chem.* **2013**, *730*, 57-62.

(12) Schulz, S. Low-Valent Organometallics - Synthesis, Reactivity, and Potential Applications. *Chem. Eur. J.* **2010**, *16*, 6416-6428.

(13) Nagendran, S.; Roesky, H. W. The Chemistry of Aluminum(I), Silicon(II), and Germanium(II). *Organometallics* **2008**, *27*, 457-492.

(14) Gemel, C.; Steinke, T.; Cokoja, M.; Kempter, A.; Fischer, Roland A. Transition Metal Chemistry of Low Valent Group 13 Organyls. *Eur. J. Inorg. Chem.* **2004**, *2004*, 4161-4176.

(15) Akrivos, P. D.; Katsikis, H. J.; Koumoutsi, A. Low Valent Coinage Metal Coordination Compounds with Group 15, 16 and 17 Donors. *Coord. Chem. Rev.* **1997**, *167*, 95-204.

(16) Melen, R. L. Frontiers in Molecular p-Block Chemistry: From Structure to Reactivity. *Science* **2019**, *363*, 479-484.

(17) Légaré, M.-A.; Bélanger-Chabot, G.; Dewhurst Rian, D.; Welz, E.; Krummenacher, I.; Engels, B.; Braunschweig, H. Nitrogen Fixation and Reduction at Boron. *Science* **2018**, *359*, 896-900.

(18) Rösch, B.; Gentner, T. X.; Langer, J.; Färber, C.; Eyselein, J.; Zhao, L.; Ding, C.; Frenking, G.; Harder, S. Dinitrogen Complexation and Reduction at Low-Valent Calcium. *Science* **2021**, *371*, 1125-1128.

(19) Zhong, M.; Sinhababu, S.; Roesky, H. W. The Unique β-Diketiminate Ligand in Aluminum(I) and Gallium(I) Chemistry. *Dalton Trans.* **2020**, *49*, 1351-1364.

(20) Liu, Y.; Li, J.; Ma, X.; Yang, Z.; Roesky, H. W. The Chemistry of Aluminum(I) with β-Diketiminate Ligands and Pentamethylcyclopentadienyl-Substituents: Synthesis, Reactivity and Applications. *Coord. Chem. Rev.* **2018**, *374*, 387-415.

(21) Wehmschulte, R. J., Low Valent Organoaluminum (+I, +II) Species. In *Modern Organoaluminum Reagents: Preparation, Structure, Reactivity and Use*, Woodward, S.; Dagorne, S., Eds. Springer-Verlag Berlin Heidelberg: Berlin, Heidelberg, 2013; Vol. 41, pp 91 - 124.

(22) Roesky, H. W.; Kumar, S. S. Chemistry of Aluminium(I). *Chem. Commun.* **2005**, 4027-4038.

(23) Sudheendra Rao, M. N.; Roesky, H. W.; Anantharaman, G. Organoaluminum Chemistry with Low Valent Aluminum - Recent Developments. *J. Organomet. Chem.* **2002**, *646*, 4-14.

(24) Hicks, J.; Vasko, P.; Goicoechea, J. M.; Aldridge, S. The Aluminyl Anion: A New Generation of Aluminium Nucleophile. *Angew. Chem. Int. Ed.* **2021**, *60*, 1702-1713.

(25) Hicks, J.; Vasko, P.; Goicoechea, J. M.; Aldridge, S. Synthesis, Structure and Reaction Chemistry of a Nucleophilic Aluminyl Anion. *Nature* **2018**, *557*, 92-95.

(26) Schwamm, R. J.; Anker, M. D.; Lein, M.; Coles, M. P. Reduction vs. Addition: The Reaction of an Aluminyl Anion with 1,3,5,7-Cyclooctatetraene. *Angew. Chem. Int. Ed.* **2019**, *58*, 1489-1493.

(27) Schwamm, R. J.; Coles, M. P.; Hill, M. S.; Mahon, M. F.; McMullin, C. L.; Rajabi, N. A.; Wilson, A. S. S. A Stable Calcium Alumanyl. *Angew. Chem. Int. Ed.* **2020**, *59*, 3928-3932.

(28) Grams, S.; Eyselein, J.; Langer, J.; Färber, C.; Harder, S. Boosting Low-Valent Aluminum(I) Reactivity with a Potassium Reagent. *Angew. Chem. Int. Ed.* **2020**, *59*, 15982-15986.

(29) Kurumada, S.; Takamori, S.; Yamashita, M. An Alkyl-Substituted Aluminium Anion with Strong Basicity and Nucleophilicity. *Nat. Chem.* **2020**, *12*, 36-39.

(30) Koshino, K.; Kinjo, R. Construction of σ-Aromatic AlB_2 Ring via Borane Coupling with a Dicoordinate Cyclic (Alkyl)(Amino)Aluminyl Anion. *J. Am. Chem. Soc.* **2020**, *142*, 9057-9062.

(31) Schwamm, R. J.; Hill, M. S.; Liu, H.-Y.; Mahon, M. F.; McMullin, C. L.; Rajabi, N. A. Seven-Membered Cyclic Potassium Diamidoalumanyls. *Chem. Eur. J.* **2021**, *27*, 14971-14980.

(32) Hicks, J.; Vasko, P.; Goicoechea, J. M.; Aldridge, S. Reversible, Room-Temperature C–C Bond Activation of Benzene by an Isolable Metal Complex. *J. Am. Chem. Soc.* **2019**, *141*, 11000-11003.

(33) Gentner, T. X.; Mulvey, R. E. Alkali-Metal Mediation: Diversity of Applications in Main-Group Organometallic Chemistry. *Angew. Chem. Int. Ed.* **2021**, *60*, 9247-9262.

(34) Evans, M. J.; Anker, M. D.; McMullin, C. L.; Neale, S. E.; Coles, M. P. Dihydrogen Activation by Lithium- and Sodium-Aluminyls. *Angew. Chem. Int. Ed.* **2021**, *60*, 22289-22292.

(35) Roy, M. M. D.; Hicks, J.; Vasko, P.; Heilmann, A.; Baston, A.-M.; Goicoechea, J. M.; Aldridge, S. Probing the Extremes of Covalency in M−Al bonds: Lithium and Zinc Aluminyl Compounds. *Angew. Chem. Int. Ed.* **2021**, *60*, 22301-22306.

(36) Fulmer, G. R.; Miller, A. J. M.; Sherden, N. H.; Gottlieb, H. E.; Nudelman, A.; Stoltz, B. M.; Bercaw, J. E.; Goldberg, K. I. NMR Chemical Shifts of Trace Impurities: Common Laboratory

Solvents, Organics, and Gases in Deuterated Solvents Relevant to the Organometallic Chemist. *Organometallics* **2010**, *29*, 2176-2179.

(37) Cordero, B.; Gómez, V.; Platero-Prats, A. E.; Revés, M.; Echeverría, J.; Cremades, E.; Barragán, F.; Alvarez, S. Covalent Radii Revisited. *Dalton Trans.* **2008**, 2832-2838.

(38) Groom, C. R.; Bruno, I. J.; Lightfoot, M. P.; Ward, S. C. The Cambridge Structural Database. *Acta Cryst.* **2016**, *B72*, 171-179. CSD Version 5.42 updates (Sep 2021).

(39) Agou, T.; Wasano, T.; Jin, P.; Nagase, S.; Tokitoh, N. Syntheses and Structures of an "Alumole" and Its Dianion. *Angew. Chem. Int. Ed.* **2013**, *52*, 10031-10034.

(40) Uhl, W.; Er, E.; Hübner, O.; Himmel, H.-J. Monomere versus Dimere Dialkylaluminiumalkinide R_2Al-C≡C-R′ – Dreifach Koordinierte Aluminiumatome Gebunden an C≡C-Dreifachbindungen. *Z. Anorg. Allg. Chem.* **2008**, *634*, 2133-2139.

(41) Fryzuk, M. D.; Giesbrecht, G. R.; Rettig, S. J. Synthesis, Characterization, and Solution Dynamics of Alkali-Metal Chloride, Aluminate, and Borate Adducts of the Tridentate Amido Diphosphine Ligand Precursor $LiN(SiMe_2CH_2PPr^i_2)_2$. *Organometallics* **1997**, *16*, 725-736.

(42) Nöth, H.; Schlegel, A.; Knizek, J.; Schwenk, H. Di-, Tri-, and Tetranuclear Alkoxyaluminum Hydrides. *Angew. Chem., Int. Ed. Engl.* **1997**, *36*, 2640-2643.

(43) Schumann, H.; Hummert, M.; Lukoyanov, A. N.; Fedushkin, I. L. Sodium Cation Migration Above the Diimine π-System of Solvent Coordinated dpp-BIAN Sodium Aluminum Complexes (dpp-BIAN=1,2-Bis[(2,6-diisopropylphenyl)imino]acenaphthene). *Chem. Eur. J.* **2007**, *13*, 4216-4222.

(44) Wright, R. J.; Brynda, M.; Power, P. P. Synthesis and Structure of the "Dialuminyne" $Na_2[Ar'AlAlAr']$ and $Na_2[(Ar''Al)_3]$: Al–Al Bonding in Al_2Na_2 and Al_3Na_2 Clusters. *Angew. Chem. Int. Ed.* **2006**, *45*, 5953-5956.

(45) Rahm, M.; Hoffmann, R.; Ashcroft, N. W. Atomic and Ionic Radii of Elements 1–96. *Chem. Eur. J.* **2016**, *22*, 14625-14632.

(46) Jin, K. J.; Collum, D. B. Solid-State and Solution Structures of Glycinimine-Derived Lithium Enolates. *J. Am. Chem. Soc.* **2015**, *137*, 14446-14455.

(47) Jaiswal, K.; Prashanth, B.; Bawari, D.; Singh, S. Bis(phosphinimino)amide Supported Borondihydride and Heteroleptic Dihalo Compounds of Group 13. *Eur. J. Inorg. Chem.* **2015**, *2015*, 2565-2573.

(48) Armstrong, David R.; Davies, Robert P.; Haigh, R.; Hendy, Mark A.; Raithby, Paul R.; Snaith, R.; Wheatley, Andrew E. H. A Solid-State, Solution, and Theoretical Structural Study of Kinetic and Thermodynamic Lithiated Derivatives of a Simple Diazomethane and Their Reactivities Towards Aryl Isothiocyanates. *Eur. J. Inorg. Chem.* **2003**, *2003*, 3363-3375.

(49) Jones, C.; Junk, P. C.; Leary, S. G.; Smithies, N. A. Syntheses and Structural Studies of Lithium Complexes of 2-amino-6-methylpyridine*J. Chem. Soc., Dalton Trans.* **2000**, 3186-3190.

(50) Hitchcock, P. B.; Lappert, M. F.; Wang, Z.-X. Reactions of α-Lithiated Phosphinimines with PhCN; the crystal structure of $[K\{N(H)C(Ph)C(H)P(Ph)_2NSiMe_3\}(tmen)]_2$ (tmen = $Me_2NCH_2CH_2NMe_2$). *J. Chem. Soc., Dalton Trans.* **1997**, 1953-1956.

(51) Von Pilgrim, M.; Mondeshki, M.; Klett, J. [Bis(Trimethylsilyl)Methyl]Lithium and -Sodium: Solubility in Alkanes and Complexes with O- and N- Donor Ligands. *Inorganics* **2017**, *5*, 39.

(52) Izod, K.; McFarlane, W.; Tyson, B. V.; Clegg, W.; Harrington, R. W.; Liddle, S. T. Alkali Metal-Mediated Schlenk Dimerization of a Phosphorus-Substituted Alkene. Synthesis and Crystal Structures of Li, Na, and K Derivatives of a Phosphorus-Stabilized Butane-1,4-diide Ligand. *Organometallics* **2003**, *22*, 3684-3690.

(53) Elsen, H.; Färber, C.; Ballmann, G.; Harder, S. $LiAlH_4$: From Stoichiometric Reduction to Imine Hydrogenation Catalysis. *Angew. Chem. Int. Ed.* **2018**, *57*, 7156-7160.

(54) Pollard, V. A.; Orr, S. A.; McLellan, R.; Kennedy, A. R.; Hevia, E.; Mulvey, R. E. Lithium Diamidodihydridoaluminates: Bimetallic Cooperativity in Catalytic Hydroboration and Metallation Applications. *Chem. Commun.* **2018**, *54*, 1233-1236.

(55) Sattler, E.; Szilvási, T.; Matern, E.; Bombicz, P.; Gamer, M.; Okrut, A.; Kovács, I. Investigations of $LiP(SiMe_2CH_2SiMe_3)–P\textit{t}Bu_2$, the Surprising Byproduct in the Metalation of $(Me_3Si)2P–P\textit{t}Bu_2$. *Eur. J. Inorg. Chem.* **2017**, *2017*, 5521-5528.

(56) Uhl, W.; Rösener, C.; Layh, M.; Hepp, A. Treatment of a Methylene-Bridged Dialuminium Compound with Lithium Alkanides and Alkynides - Single vs. Twofold Terminal Coordination. *Z. Anorg. Allg. Chem.* **2012**, *638*, 1746-1754.

(57) Gabbai, F. P.; Chirik, P. J.; Fogg, D. E.; Meyer, K.; Mindiola, D. J.; Schafer, L. L.; You, S.-L. An Editorial About Elemental Analysis. *Organometallics* **2016**, *35*, 3255-3256.

Table of Contents

Control over the extent of the bonding between aluminum and the group 1 metals in lithium, sodium and potassium aluminyls has been demonstrated. Non-solvated, contacted dimeric pairs [**M**{Al(NON^{Dipp})}]$_2$ are converted to monomeric ion pairs containing highly polarized Al$^{\delta-}$–**M**$^{\delta+}$ bonds using THF (**M** = Li, Na) or TMEDA (**M** = Li, Na, K). Separated ion pairs containing isolated [Al(NON^{Dipp})]$^-$ anions and sequestered cations are accessed for [Li(TMEDA)$_2$]$^+$ and [**M**(2.2.2)crypt]$^+$ (**M** = Na, K).